

Applications of nanomaterials based on magnetite and mesoporous silica on the selective detection of zinc ion in live cell imaging

Roghayeh Sadeghi Erami^{1,2}, Karina Ovejero³, Soraia Meghdadi¹, Marco Filice^{3,4,5*}, Mehdi Amirnasr^{1,*}, Antonio Rodríguez-Diéguez,⁶ M. Ulagares De La Orden⁷ and Santiago Gómez-Ruiz^{2,*}

¹ Department of Chemistry, Isfahan University of Technology, Isfahan 84156-83111, Iran; romochem@gmail.com (R.S.E.); smeghdad@cc.iut.ac.ir (S.M.)

² Departamento de Biología y Geología, Física y Química Inorgánica, ESCET, Universidad Rey Juan Carlos, Calle Tulipán s/n, E-28933 Móstoles, Madrid, Spain

³ National Research Centre for Cardiovascular Disease (CNIC), Melchor Fernández Almagro, 3, 28029 Madrid, Spain; k.ovejero94@gmail.com

⁴ Dept. of Chemistry in Pharmaceutical Sciences, Faculty of Pharmacy, Complutense University (UCM), Plaza Ramón y Cajal s/n, 28040 Madrid, Spain

⁵ Biomedical Research Networking Center for Respiratory Diseases (CIBERES), Melchor Fernández Almagro, 3, 28029 Madrid, Spain

⁶ Departamento de Química Inorgánica, Facultad de Ciencias, Campus de Fuentenueva. Avda. Fuentenueva s/n, 18071 Granada, Spain; antonio5@ugr.es

⁷ Departamento de Química Orgánica I, E. U. Óptica, Universidad Complutense de Madrid, Arcos de Jalón, s/n, 28037 Madrid, Spain; mariula@quim.ucm.es

* Correspondence: mfilice@ucm.es (M.F.); amirnasr@cc.iut.ac.ir (M.A.); santiago.gomez@urjc.es (S.G.-R.); Tel.: +34-91-394-1751 (M.F.); +98-31-3391-2351 (M.A.); +34-91-488-8507 (S.G.-R.);

Fax: +98-31-3391-2350 (M.A.); +34-91-488-8143 (S.G.-R.)

Table of Contents – Supporting Information

1. Additional data of the characterizations of FMNPs and FMSNs	1
2. Description of the benign Synthesis of 2(2-hydroxyphenyl)benzothiazole (hpbtz)	6
References	8

1. Additional data of the characterizations of FMNPs and FMSNs

The thermal behavior of magnetite- and silica-based materials were investigated by thermogravimetric analysis (Figs. S1 and S2) and the resulting data are given in Table 3 of the manuscript. As shown in the thermograms of a-e (Fig. S1), the weight loss below 150 °C is characteristic of the adsorbed water and residual organic solvent in the magnetite-based materials. Moreover, MNPs and FMNPs exhibit an additional weight loss between around 190 to 450 °C. This step with 1.31, 2.54, 1.21, 5.41 and 8.73% weight loss for a to e, respectively, is attributed to the removal of organic moieties (including ethylene glycol, ascorbic acid and **hpbtz**) on the nanoparticles surface. As it is clear from the thermal analysis data, **Fe₃O₄-C@hpbtz** (d) has the highest weight loss compared to the other magnetite-based materials due to its higher organic content. However, the thermogram of e shows a weight loss between 190 to 450 °C including three steps presumably due to the decomposition of different organic fractions composed of ascorbic acid, as stabilizing agent, **hpbtz** ligand and residual ethylene glycol grafted on the nanoparticles surface. Fig. S2

presents the thermogravimetric analysis of MSNs and MSN-NEt₃-IPTMS-hpbtz-**f1** (labeled as g and f, respectively). The initial weight loss up to 190 °C in g and f is assigned to the desorption of residual water molecules trapped in the silica porous structure. The next main weight loss at above 200°C is probably due to the decomposition of the organic fractions. It seems that the main weight loss with about 1.44% in the thermogram of MSNs is originated from the condensation of silanol groups of the material as it is mainly observed above 550 °C. Moreover, the amount of the immobilized organic fractions onto MSN-NEt₃-IPTMS-hpbtz-**f1** is estimated to be 18.54 %, corresponding to the presence of CTAB, IPTMS and **hpbtz** ligand.

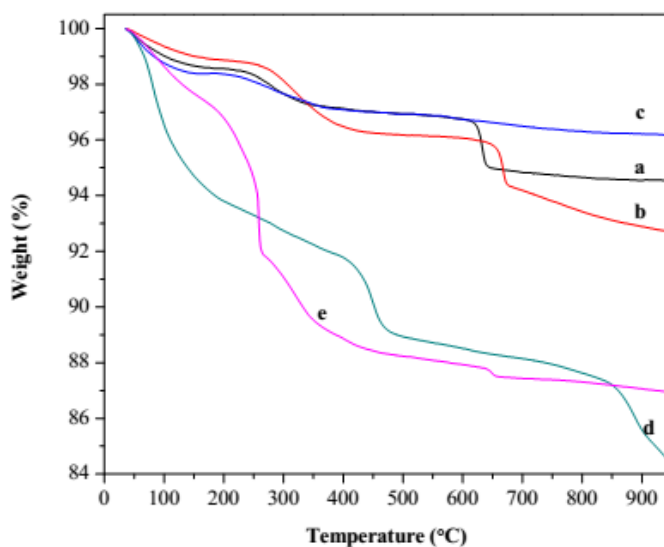


Figure S1. TGA thermograms of a) Fe₃O₄-H, b) Fe₃O₄-H@hpbtz, c) Fe₃O₄-C, d) Fe₃O₄-C@hpbtz and e) Fe₃O₄@hpbtz using a heating rate of 20 °C min⁻¹ in nitrogen.

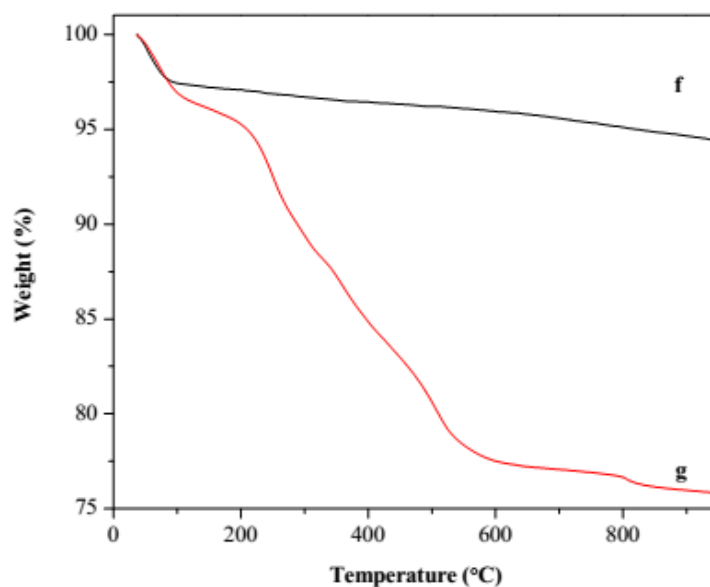


Figure S2. TGA thermograms of f) MSNs and g) MSN-Et₃N-IPTMS-hpbtz-f1, using a heating rate of 20 °C min⁻¹ in nitrogen.

The introduction of the coupling agents and hpbtz fluorophore onto the magnetite and silica nanoparticles was further confirmed by FT-IR and UV-vis spectral analysis. The FT-IR spectra of FMNPs and FMSNs are presented in (Figs. S3 and S4). For the Fe₃O₄-H, Fe₃O₄-C, Fe₃O₄-H@hpbtz, Fe₃O₄-C@hpbtz, and Fe₃O₄@hpbtz (Fig. S3), there are two main bands at 570 cm⁻¹ attributed to the vibration of Fe-O and a broad band at ca. 3430 cm⁻¹ corresponds to the stretching of the O-H groups on the external NPs surface, indicating the magnetite formation. In addition, two bands at around 1630 and 1380 cm⁻¹ are assigned to the bending vibration and deformation of the H-O-H of physically adsorbed water, respectively. In the spectrum of hpbtz (Fig. S3c), there are two characteristic bands at 1600 and 1580 cm⁻¹ assigned to the (C=C) and (C=N) stretching vibrations and around 1487 and 1439 cm⁻¹ characteristic of the (C=C) stretching and (C-H) bending vibrations of the benzothiazole moiety [1]. The first two characteristic bands of hpbtz, i.e. azomethine (C=N) and (C=C) stretching vibrations appear in the nearly similar positions in the functionalized materials spectra (Fig S3 d, e, and f). In the S1f spectrum, the C=O stretching bands of vitamin C and its oxidized form are absent indicating that the carbonyl group is modified by coordinating to the Fe center on the MNPs surface [2,3]. The presence of low intensity peaks around 1400 cm⁻¹ are also assigned to the aromatic C-H bending vibrations of the benzothiazole moiety in S3 d, e and f [4].

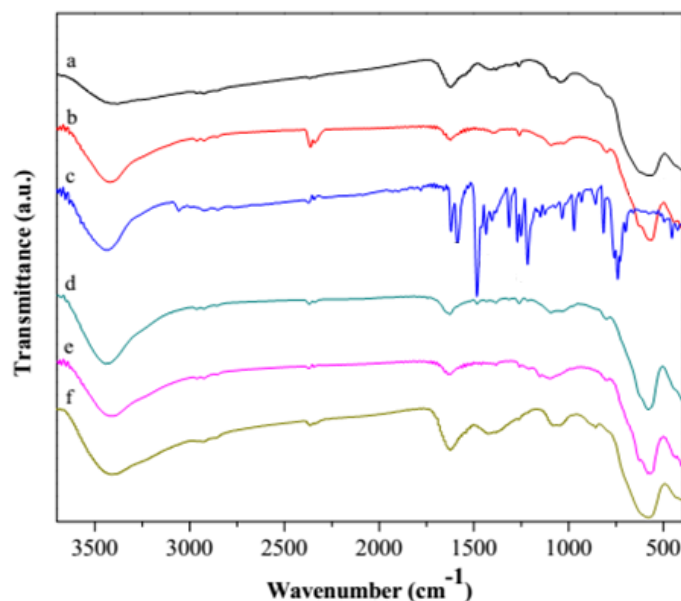


Figure S3. FT-IR spectra of FMNPs a) Fe₃O₄-H, b) Fe₃O₄-C, c) hpbtz ligand, d) Fe₃O₄-H@hpbtz, e) Fe₃O₄-C@hpbtz and f) Fe₃O₄@hpbtz.

The FT-IR spectra of MSNs and FMSNs: MSN-Et₃N-IPTMS-hpbtz-f1, MSN-pyridine-IPTMS-hpbtz-f2, MSN-NaOH-IPTMS-hpbtz-f3, MSN-Et₃N-NCO-hpbtz-e1, MSN-pyridine-NCO-hpbtz-e2, MSN-NaOH-NCO-hpbtz-e3 and hpbtz ligand are shown in Fig. S4. The FT-IR spectrum of MSNs (Fig. S4, a) shows characteristic band at 1630 cm⁻¹ assigned to O-H stretching vibration of the remaining physisorbed water molecules. As a result of mesoporous silica formation, a strong peak with maximum near 1090 cm⁻¹, corresponding to Si-O-Si stretching vibrations appears. Two additional bands appearing at 970 and 804 cm⁻¹ are due to Si-O-H and Si-O-Si bending vibrations. The IPTMS and ICTES functionalized materials (Fig. S4, b-g) display additional absorption bands at around 2930 and 2980 cm⁻¹ due to the ν(C-H) stretching

vibrations in the propyl chains of organosilane coupling agents. In the **S4 c, e and g** spectra the bending vibration of amidic N-H appears at 1580 cm^{-1} . Moreover, the disappearance of the band at 2225 cm^{-1} is attributed to the stretching vibration of NCO, and the appearance of a new carboxylic band at 1680 cm^{-1} indicate that the reaction between the isocyanate group in ICTES and hydroxyl of hpbtz occurred successfully [5,6]. However, the strong Si-O-Si stretching vibrations near to 1090 cm^{-1} attenuates the intensity of the characteristic bands of hpbtz which are expected to appear at around 1400 cm^{-1} .

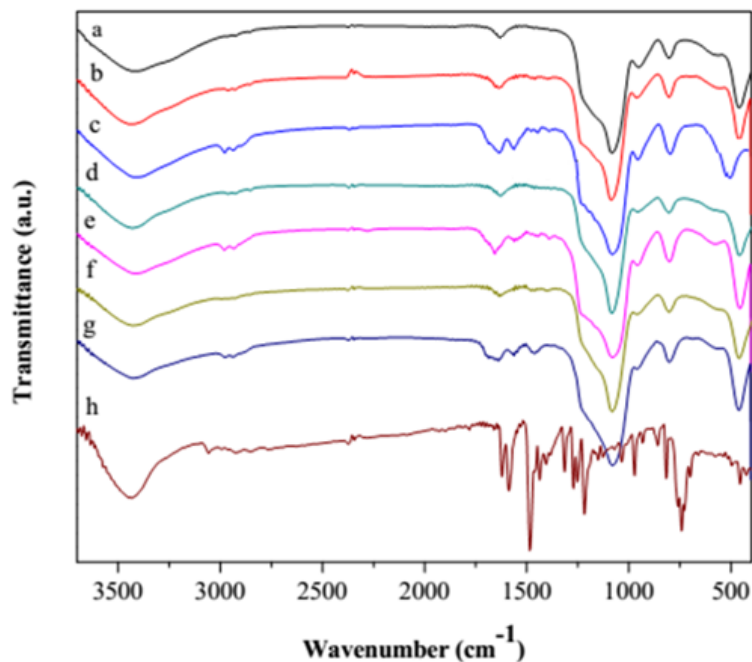


Figure S4. FT-IR spectra of a) MSNs and FMSNs: b) MSN-Et₃N-IPTMS-hpbtz-f1, c) MSN-Et₃N-NCO- hpbtz -e1, d) MSN-pyridine-IPTMS-hpbtz-f2, e) MSN-pyridine-NCO-hpbtz-e2, f) MSN-NaOH-IPTMS-hpbtz-f3, g) MSN-NaOH-NCO-hpbtz-e3 and h)hpbtz ligand.

The UV-vis spectra of FMNPs and FMSNs are presented in (**Figs. S5 and S6**). **Fig. S5** shows a comparative UV-vis study of colloidal dispersion of MNPs and their functionalization with hpbtz at a concentration of 2 mg mL^{-1} in ethanol. The spectrum of pure hpbtz dissolved in ethanol is also given for comparison. The magnetite nanoparticles ($\text{Fe}_3\text{O}_4\text{-H}$ and $\text{Fe}_3\text{O}_4\text{-C}$) spectra show a broad absorption band at around 350 nm , corresponding to the charge transfer from oxide to iron Fe^{3+} d orbitals in the octahedral and tetrahedral sites [7]. The absorption spectrum of hpbtz shows three absorption bands at 216 , 288 and 336 nm corresponds to the intra ligand charge transitions [8].

From the comparison between the absorption spectra of hpbtz and FMNPs in **Fig. S5** it is clear that the incorporation of hpbtz onto the magnetite nanoparticles leads to a slight red shift in the ligand absorption bands. This is a good evidence for effective coordination of the ligand to the MNPs. Furthermore, a new broad band appears at around 400 nm in the $\text{Fe}_3\text{O}_4\text{-H@hpbtz}$, $\text{Fe}_3\text{O}_4\text{-C@hpbtz}$ and $\text{Fe}_3\text{O}_4\text{@hpbtz}$ spectra due to the ligand to metal charge transfer from the surface bound ligand to the metal core.

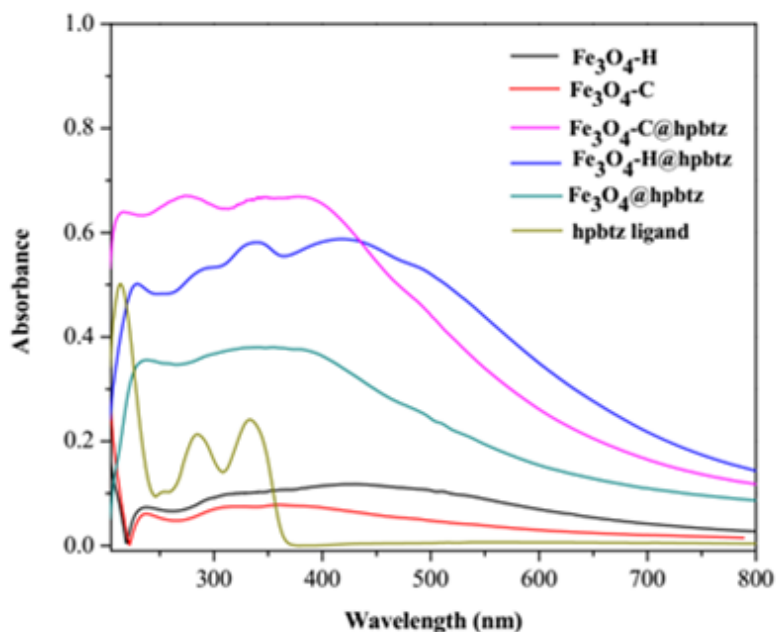


Figure S5. UV-vis spectra of MNPs, FMNPs and hpbtz ligand at a concentration of 2 mg mL⁻¹.

Considering the higher ligand quantity in mmol per gram of material prepared in post functionalization with IPTMS, and determined by XRF analysis data (**Table 2**), comparative UV-vis spectra of colloidal dispersion of MSN and FMSNs (f1-f3) at a concentration of 2 mg mL⁻¹ in ethanol have been recorded (**Fig. S6**). The spectrum of pure hpbtz dissolved in ethanol is also given for comparison (**Fig S6, e**). For mesoporous silica nanoparticles there are two characteristic bands at 223 and 288 nm correspond to Si-O ligand to metal charge transfer. As shown in **Figs. S6, b, c and d**, the spectra of functionalized mesoporous materials show characteristic absorption bands from hpbtz and correspond to the intraligand transitions.

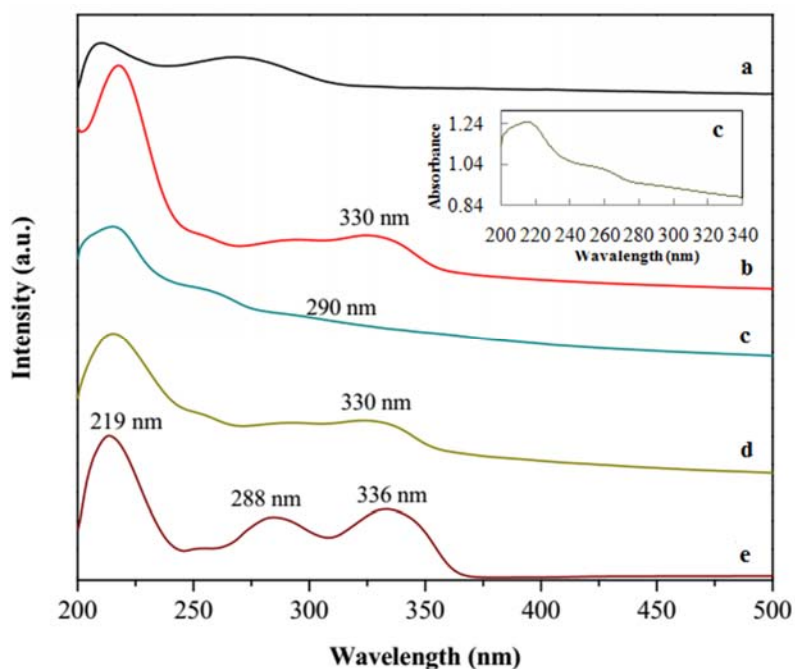
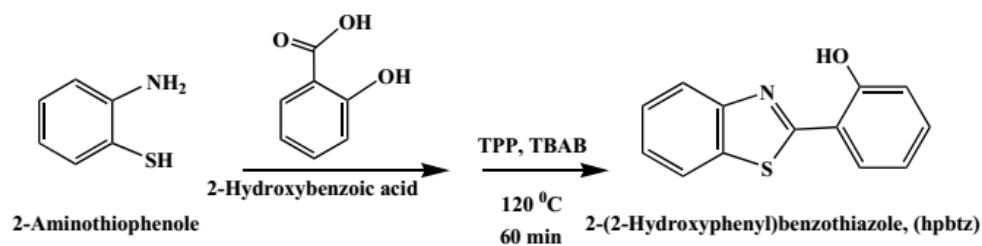


Figure S6. UV-vis spectra of MSNs and FMSNs: a) MSNs, b) MSN-Et₃N-IPTMS-hpbtz-f1, c) MSN-pyridine-IPTMS-hpbtz-f2, d) MSN-NaOH-IPMS-hpbtz-f3, at a concentration of 2 mg mL⁻¹ and e) hpbtz ligand (10⁻⁵ M). [inset: c at a higher concentration].

2. Description of the benign Synthesis of 2-(2-hydroxyphenyl)benzothiazole (hpbtz)

The ligand hpbtz was synthesized by a benign and environmentally friendly method that we have recently reported using the ionic liquid tetrabutylammonium bromide (TBAB) as the reaction medium [9]. Briefly, as shown in **Scheme S1**, a mixture of triphenyl phosphite (TPP) (1.55 g, 5 mmol), tetrabutylammonium bromide (TBAB) (1.66 g, 5 mmol), 2-aminothiophenol (0.625 g, 5 mmol) and 2-hydroxybenzoic acid (0.69 g, 5 mmol) in a 25 mL round bottomed flask was placed in an oil bath. The solution was stirred for 60 min at 120 °C. The product precipitated from the viscous solution by adding MeOH, and the resulting solid was filtered off and washed with cold MeOH. Yield: 76 mg, 92%, ¹H NMR: Figs. S7-S8.



Scheme S1. Synthetic method for the preparation of 2-(2-hydroxyphenyl)benzothiazole (hpbtz).

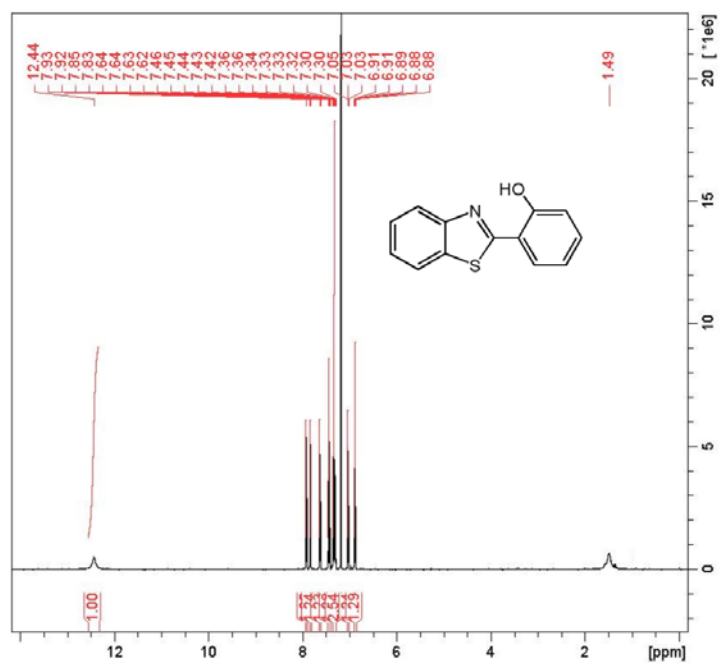


Figure S7. ^1H NMR spectrum of Hpbtz

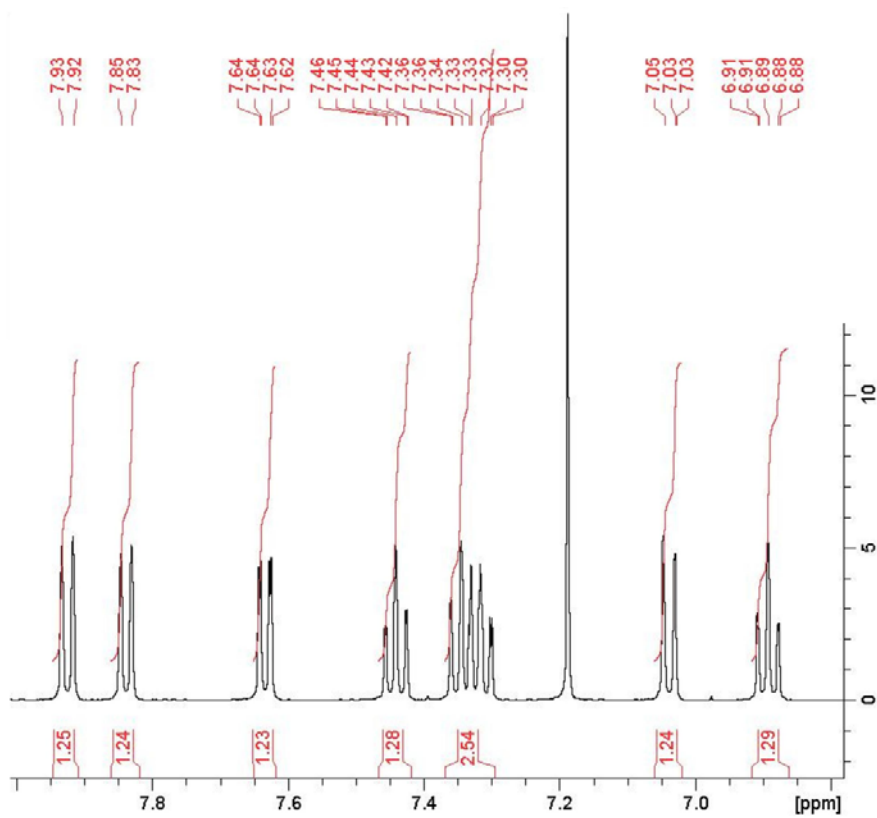


Figure S8. ^1H NMR spectrum of Hpbtz

References

1. Li, Z.; Dellali, A.; Malik, J.; Motevalli, M.; Nix, R.M.; Olukoya, T.; Peng, Y.; Ye, H.; Gillin, W.P.; Hernandez, I.; Wyatt, P.B. Luminescent Zinc(II) Complexes of Fluorinated Benzothiazol-2-yl Substituted Phenoxide and Enolate Ligands. *Inorg. Chem.* **2013**, *52*, 1379–1387, DOI: 10.1021/ic302063u.
2. Li, Z.; Chen, H.; Bao, H.; Gao, M. One-Pot Reaction to Synthesize Water-Soluble Magnetite Nanocrystals. *Chem. Mater.* **2004**, *16*, 1391–1393, DOI: 10.1021/cm035346y.
3. Li, Z.; Wei, L.; Gao, M.; Lei, H. One-Pot Reaction to Synthesize Biocompatible Magnetite Nanoparticles. *Adv. Mater.* **2005**, *17*, 1001–1005, DOI: 10.1002/adma.200401545.
4. Nakamoto, K. *Infrared and Raman spectrum of Inorganic and Coordination Compounds*, fifth ed., John Wiley and Sons Inc., New York, 1997, DOI: 10.1002/9780470405840.
5. Saleh, T.A. The influence of treatment temperature on the acidity of MWCNT oxidized by HNO₃ or a mixture of HNO₃/H₂SO₄. *Appl. Surf. Sci.* **2011**, *257*, 7746–7751, DOI: 10.1016/j.apsusc.2011.04.020.
6. Gupta, V.K.; Agarwal, S.; and Saleh, T.A. *J. Hazard. Mater.* **2011**, *185*, 17–23, DOI: 10.1016/j.jhazmat.2010.08.053.
7. Sherman, D.M.; Waite, T.D. Electronic spectra of Fe³⁺ oxides and oxide hydroxides in the near IR to near UV. *Am. Mineral.* **1985**, *70*, 1262–1269.
8. Grando, S.R.; Pessoa, C.M.; Gallas, M.R.; Costa, T.M.H.; Rodembusch, F.S.; and Benvenutti, E.V. Modulation of the ESIPT Emission of Benzothiazole Type Dye Incorporated in Silica-Based Hybrid Materials. *Langmuir* **2009**, *25*, 13219–13223, DOI: 10.1021/la902242y.
9. Meghdadi, S.; Amirnasr, M.; and Ford, P.C. A robust one-pot synthesis of benzothiazoles from carboxylic acids including examples with hydroxyl and amino substituents. *Tetrahedron Lett.* **2012**, *53*, 6950–6953, DOI: 10.1016/j.tetlet.2012.10.035.